

Detecting non-linearities in data sets. Characterization of Fourier phase maps using the Weighted Scaling Indices.

Roberto A. Monetti, Wolfram Bunk, Ferdinand Jamitzky, Christoph R ath, and Gregor Morfill
*Center for Interdisciplinary Plasma Science (CIPS) Max-Planck-Institut
 f ur extraterrestrische Physik Giessenbachstr. 1, 85748 Garching, Germany*
 (Dated: 13th November 2018)

We present a methodology for detecting non-linearities in data sets based on the characterization of the structural features of the Fourier phase maps. A Fourier phase map is a $2D$ set of points $M = \{(\phi_{\vec{k}}, \phi_{\vec{k}+\vec{\Delta}})\}$, where $\phi_{\vec{k}}$ is the phase of the k -mode of the Fourier transform of the data set and $\vec{\Delta}$ a phase shift. The information thus rendered on this space is analyzed using the spectrum of weighted scaling indices to detect phase coupling at any scale $\vec{\Delta}$. We propose a statistical test of significance based on the comparison of the properties of phase maps created from both the original data and surrogate realizations. We have applied our method to the Lorenz system and the logarithmic stock returns of the Dow Jones index. Applications to higher dimensional data are straightforward. The results indicate that both the Lorenz system and the Dow Jones time series exhibit significant signatures of non-linear behavior.

PACS numbers: 05.45.-a 02.50.-r 89.20.-a

The first step in the characterization of a data set is usually the calculation of the 'linear properties', i.e. the power spectrum and the amplitude distribution. However, in many cases the estimation of higher-order properties is required. For instance, given an image it is possible to generate from it a new one by shuffling the Fourier phases. The resulting image may look different although the phase shuffling process preserves the power spectrum of the original one. Then, the Fourier phases contain information which is beyond the linear properties of the data, the so-called non-linear properties. A challenging problem is then the extraction and characterization of the information contained in the Fourier phases. The phases are a powerful indicator of the structure of a data set. It was early noticed that an image synthesized by keeping the Fourier amplitudes and changing the Fourier phases retains almost no feature of the original image. However, image synthesized by keeping the Fourier phases and changing the Fourier amplitudes conserve most of the structure observed on the original image [1]. Studies of Fourier phase coupling are mostly found in the field of astrophysics where the aim is to characterize the growth of large-scale structure in the universe [2, 3] and to test for non-Gaussian signatures in the Cosmic Microwave Radiation Background [4]. Except for these few cases, the methods to test for non-linearities have never focused on the analysis of phase correlations, although some of them are based on phase randomization procedures. This is probably due to difficulties in constructing good estimates out of phases since they are circular quantities (defined modulo 2π) and not translational invariant, as was already noted in [2, 3, 4]. In this work, we present a method to analyze the Fourier phase information based on the assessment of the so called 'Fourier Phase Maps'. First, the method of surrogates [5, 6, 7, 8, 9] is used to generate an ensemble of data sets which mimic the linear properties of the original data set however wiping out higher-order correlations. Then, we generate for

both the original data set and the surrogate data phase maps which are subsequently characterized by means of the spectrum of weighted scaling indices [10, 11]. If the computed measure for the original data is significantly different from the value obtained for the surrogate data set, one can infer that the data were generated by a non-linear process.

Consider an N -dimensional data set $\{\vec{x}_i\}$ with Fourier phases $\{\phi_{\vec{k}}\}$. Given a phase shift $\vec{\Delta}$ a phase map is defined as the two dimensional set of points $M = \{(\phi_{\vec{k}}, \phi_{\vec{k}+\vec{\Delta}})\}$. All possible wave numbers \vec{k} are considered up to the Nyquist frequency so as not to include redundant information. The phase maps possess attracting features which are useful to reveal non-linear properties. First, it is well known that the Fourier transform of a random Gaussian variable has uncorrelated and uniformly distributed phases in the interval $[-\pi, \pi]$. Then, the plot of the phase map generated by such a variable will be a uniform point distribution on the square bounded by $y = \pm\pi$ and $x = \pm\pi$. Here, we generate surrogate data sets using the iterative amplitude adjusted Fourier transform algorithm (ITAAFT) [7, 8]. By means of this method, we generate surrogate data sets which keep the same amplitude distribution in real space and power spectrum of the original data set however destroying higher-order correlations. It has been recently demonstrated that this algorithm can be generalized for two and three dimensional data sets [12, 13]. The surrogate method destroys higher-order properties by means of a phase randomization procedure. Thus, we expect the phase maps of surrogate data to be more uniform. This is actually the phase map feature which will be characterized in order to develop a test for non-linearities.

We have used the Scaling Index Method (SIM) to quantify the structural features of the phase maps. This technique which was inspired in the analysis of nonlinear systems [14, 15] has been successfully applied in different fields of research, ranging from astrophysical to medical

applications [10, 11, 13, 16, 17]. The SIM characterizes the structural features of a point distribution by means of the analysis of its local scaling behavior.

We first define a local weighted cumulative point distribution ρ as $\rho(\vec{x}_i, R) = \sum_j s_R(d(\vec{x}_i, \vec{x}_j))$, where $s_R(\bullet)$ denotes a kernel function which depends on the scale parameter R and a distance measure $d(\bullet)$. In principle, any differentiable kernel function and any distance measure can be used. The weighted scaling indices $\alpha(\vec{x}_i, R)$ are then obtained by calculating the logarithmic derivative of $\rho(\vec{x}_i, R)$ with respect to R ,

$$\alpha(\vec{x}_i, R) = \frac{\partial \log \rho(\vec{x}_i, R)}{\partial \log R} = \frac{R}{\rho} \frac{\partial}{\partial R} \rho(\vec{x}_i, R). \quad (1)$$

We use the Euclidean norm as distance measure and a set of exponential shaping functions. So, the expression for ρ simplifies to $\rho(\vec{x}_i, R) = \sum_j e^{-(\frac{d_{ij}}{R})^q}$, where $d_{ij} = \|\vec{x}_i - \vec{x}_j\|$. The exponent q controls the weighting of points according to their distance to the point where α is calculated. In this study, we use $q = 2$. The weighted scaling indices can then be written as

$$\alpha(\vec{x}_i, R) = \frac{\sum_j 2(\frac{d_{ij}}{R})^2 e^{-(\frac{d_{ij}}{R})^2}}{\sum_j e^{-(\frac{d_{ij}}{R})^2}}. \quad (2)$$

It should be noted that the use of shaping functions has two advantages, namely (i) one obtains an analytical expression for $\alpha(\vec{x}_i, R)$, and (ii) the scaling region is only determined by the parameter R . The scaling-index α_i characterizes the structural surrounding of \vec{x}_i . The probability $P(\alpha)d\alpha = \text{Prob}(\alpha \in [\alpha, \alpha + d\alpha])$ is therefore a statistical measure of the distribution of elementary structural components. The choice of the scaling region is not a trivial task and is crucial to obtain meaningful results using this technique. Although one is normally guided by the size of the substructures under investigation, various scaling ranges should be considered in order to obtain meaningful results.

Consider a 2D nearly uniform phase map. Since the scaling index α describes the local scaling behavior, most of the α -values will be close to $\alpha = 2$, leading to a nearly Gaussian frequency distribution centered at $\alpha = 2$. However, if the phase map contains structure, the frequency distribution will show a weaker signal around $\alpha = 2$ and new α -values will appear. The circular property of the phases implies that the embedding square is topologically equivalent to a torus. Then, the calculation of scaling indices was performed using periodic boundary conditions.

We propose a statistical test of non-linearities based on the $P(\alpha)$ spectrum. First, we generate surrogate data sets using the ITAAFT algorithm. Then, we create for the original and the surrogate data sets phase maps for phase shifts $\vec{\Delta} = \{\vec{\Delta}_1, \dots, \vec{\Delta}_m\}$, where $\vec{\Delta}_m$ is the maximum phase shift considered. The significance is defined

through the following expression

$$S(\alpha, \vec{\Delta}_l) = \frac{P_o(\alpha, \vec{\Delta}_l) - \langle P_s(\alpha, \vec{\Delta}_l) \rangle}{\sigma(P_s(\alpha, \vec{\Delta}_l))} \quad l = 1, \dots, m, \quad (3)$$

where P_o is the frequency distribution of the original phase map, and $\langle P_s \rangle$ and $\sigma(P_s)$ are the mean value and the standard deviation over the frequency distributions of the phase maps of the surrogate realizations. Equation (3) is meaningful only when $P_s(\alpha, \vec{\Delta})$ are Gaussian distributed. Although there is no proof for this statement, simulations show that mixing processes satisfy this condition. Then, S is measured in units of standard deviations. As mentioned above, we expect that the original (non-linear) data set leads to wider $P(\alpha)$ spectra while the surrogate data sets will produce $P(\alpha)$ spectra with a stronger signal around $\alpha = 2$. Then, the statistical test will give a positive result if the following condition is satisfied

$$\alpha_i \in \begin{cases} \alpha : S(\alpha, \vec{\Delta}) < -2.6 & \wedge & 1.90 \leq \alpha \leq 2.1, \\ \alpha : S(\alpha, \vec{\Delta}) > 2.6 & \wedge & \alpha \text{ elsewhere,} \end{cases} \quad (4)$$

where the value 2.6 corresponds to 1% of the quantile of the normal distribution. However, even when the condition given by Eq. (4) holds we are not certain that original and surrogate phase maps are significantly different since the scaling index is a local structure measure. In fact, every scaling index value corresponds to a region on the phase map. Thus, Eq. (4) determines the region of the phase maps where we can significantly differentiate between the original and surrogate phase maps. In the case that this region is tiny, we can not state that the original and the surrogate phase maps are significantly different. In order to address this problem, we define a new quantity Ξ through the following expression

$$\Xi(\vec{\Delta}) = \sum_{\alpha_i} P_o(\alpha_i, \vec{\Delta}), \quad (5)$$

where α_i are the α -values that satisfy Eq. (4). It should be noted that $0 \leq \Xi \leq 1$.

Thus, Ξ can be interpreted as the probability to significantly distinguish between the original and the surrogate phase maps. The probability Ξ accounts for both the significance and the extent of the region where a non-uniform structure exists.

We have applied our statistical test to two time series, namely the z -component of the Lorenz system in a chaotic regime and the logarithmic stock returns of the Dow Jones. In both cases, we generate 20 surrogates using the ITAAFT algorithm and phase shifts in the range $\Delta = \{1, \dots, 100\}$ are considered. The phase map structure is analyzed using the SIM with $R = 0.8$.

Figure 1(a) shows the time series of the z -component of the Lorenz system in a chaotic regime and a surrogate realization. One can clearly observe differences between the time series although they have not only the same amplitude distribution but also the fluctuations show the same

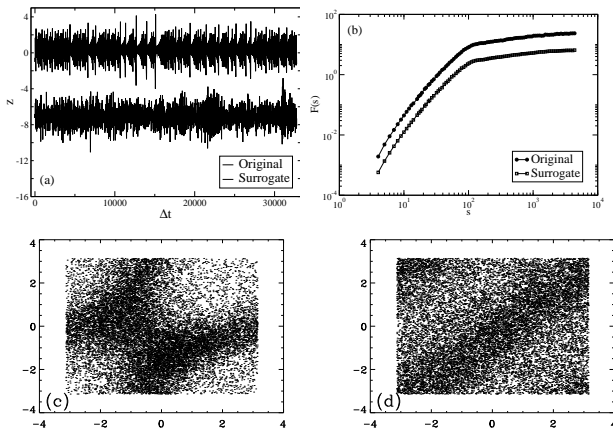


Figure 1: a) Time series of the z -component of the Lorenz system in a chaotic regime $\sigma = 10$, $r = 28$, and $b = 8/3$ and below a surrogate realization. b) Log-log plot of the scaling of the fluctuations obtained using the DFA2. The curves have been shifted to allow for comparison. c) Phase map of the Lorenz system for $\Delta = 1$. d) Phase map of a surrogate realization for $\Delta = 1$.

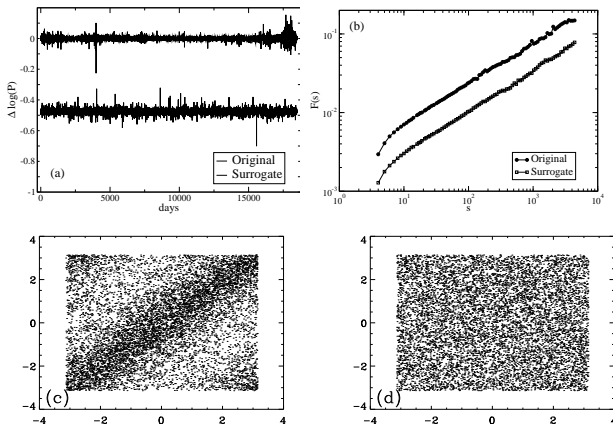


Figure 2: a) Time series of the logarithmic daily returns of the Dow-Jones for the period 1930-2003. Below, a surrogate realization. b) Log-log plot of the scaling of the fluctuations obtained using the DFA2. The curves have been shifted to allow for comparison. c) Phase map of the logarithmic returns of the Dow Jones for $\Delta = 1$. d) Phase map of a surrogate realization for $\Delta = 1$.

scaling behavior (see Fig. 1(b)). The scaling behavior of the fluctuations was obtained using the Detrended Fluctuation Analysis of order 2 (DFA2) [18]. This analysis is equivalent to the power spectrum analysis [19]. Figure 1(c) and 1(d) show phase maps for these time series. We observe that the phase map of the original time series displays high and low density regions. Although the phase map of the surrogate time series is actually more uniform, it still displays a great deal of structure. In fact, most of the the surrogate realizations of the Lorenz system gener-

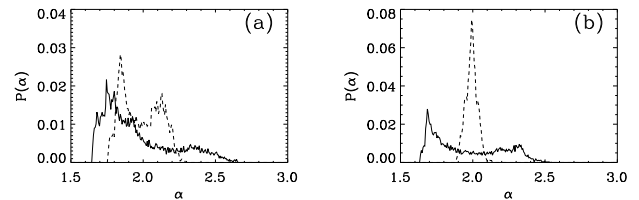


Figure 3: Frequency distribution of α -values. a) Lorenz system. b) Dow Jones index. In both cases, the full line (dashed line) indicates the original phase map (surrogate phase map).

ated using the ITAAFT algorithm display phase coupling and only some of them are free from phase correlations. Figure 3(a) shows the frequency distribution of scaling indices $P(\alpha)$ for the phase maps shown in Fig. 1. $P(\alpha)$ of the surrogate realization is narrower and more concentrated around $\alpha = 2$ which is the value expected for a uniform distribution. Figure 4(a) shows the significance for a phase shift $\Delta = 28$. We observe that a high significance is obtained for a wide range of scaling index values. The lines at $S = 20$ were included in intervals where divergencies appear. Figure 4(c) shows the probability Ξ versus Δ . It indicates that the probability to significantly differentiate between the original Lorenz time series and the surrogates oscillates around $\Xi \sim 0.40$. As expected, the Lorenz system shows signatures of non-linear behavior.

Several studies of single stock have focused on the statistical analyses of the dynamics to model the financial markets [20]. It has been noticed that economic indices exhibit a non-linear behavior [21, 22] which share some qualitative features with turbulence [23, 24, 25]. However, understanding the process that underlies the macroscopic behavior of the stocks remains at a speculative level. As noticed above, the Fourier phases are a powerful indicator of the data structure. It is then relevant to unveil and quantify the properties of the phases for stock indices. Typically, the economic indices show a correlated short-time behavior (few days) which crosses over to an uncorrelated asymptotic behavior. Figure 2(a) shows the logarithmic returns of the day to day closing price of the Dow Jones index in the period 1930-2003 [26] and a surrogate realization. Figure 2(b) shows the scaling behavior of the fluctuations. The asymptotic regime is governed by an exponent $\gamma \sim 0.5$ which is the signature of uncorrelated behavior [18]. However, the phase maps shown in Fig. 2(c) and 2(d) reveal a new scenario. The phase map for the original Dow Jones index displays a high density diagonal band and low density regions. On the other hand, the phase map for the surrogate realization looks quite uniform. In this case, the ITAAFT algorithm always generates surrogates free from phase coupling. Figure 3(b) shows the frequency distribution of scaling indices for the original and the surrogate phase maps. The spectrum of scaling indices for the phase map

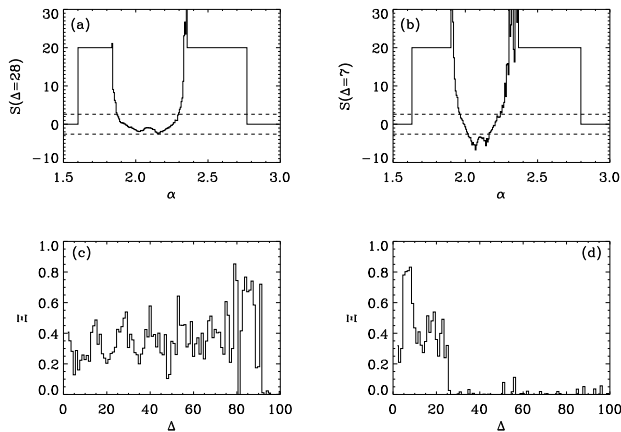


Figure 4: a) Significance for Lorenz system. The dashed horizontal lines at $S = \pm 2.6$ indicate 1% of the quantile of the normal distribution. b) Idem for the Dow Jones index. c) Probability to significantly differentiate between original and surrogate phase maps for the Lorenz system. d) Idem for the Dow Jones index.

of the surrogate realization shows a sharp peak around $\alpha = 2$. As occurred for the Lorenz system, Fig. 4(b) shows that high S values are obtained for a wide range of scaling indices. Figure 4(d) indicates that there is a high probability to significantly differentiate between the original Dow Jones index and the surrogate realizations for phase shifts up to $\Delta_c \sim 20$. Below Δ_c , the non-linearities appear to be stronger than in the Lorenz system. However, increasing the phase shift Δ the prob-

ability Ξ almost vanishes.

We have developed a new test for non-linearities based on the characterization of the Fourier phase maps using the SIM. As expected, the Lorenz system showed signatures of non-linear behavior at all Δ scales. However, we have noted that for this time series the ITAAFT algorithm is not always able to generate surrogates free from phase coupling. Then, our method could also be used to assess the quality of surrogate data sets since the performance of the generating algorithms is data dependant. Even though the fluctuations of the Dow Jones index display an uncorrelated asymptotic regime, this time series contains non-linearities which seem to be stronger than in the Lorenz system. This is probably because the ITAAFT algorithm is unable to generate surrogates free from phase coupling for the Lorenz system. Our results indicate that a novel characteristic scale of non-linearities Δ_c exists for the Dow Jones index. These findings may be useful to deeper understand the market dynamics and thus improve the results of risk assessments.

This method can be applied to higher dimensional data sets since algorithms to generate surrogates in higher dimensions are available [12, 13]. In cases where weak non-linearities may be present as in the Cosmic Microwave Background of radiation [3, 4], the use of local structure measures for the assessment of the phase maps, like the scaling indices, instead of global measures may be more appropriate since global measures may average important local details of the maps. The development of quite sensitive tests is particularly relevant for this problem where the presence or absence of non-Gaussian signatures will support different evolutionary theories of the universe.

-
- [1] A. Oppenheim and J. Lim, Proc. IEEE **69**, 529 (1981).
 [2] P. Coles and L. Chiang, Nature **406**, 376 (2000).
 [3] P. Coles, L. Chiang, and P. Naselsky, MNRAS **337**, 488 (2002).
 [4] L. Chiang, P. Naselsky, O. Verkhodanov, and M. Way, Astrophys. J. **590**, L65 (2003).
 [5] J. Theiler, S. Eubank, A. Longtin, B. Galdrikian, and J. Farmer, Physica D **590**, 77 (1992).
 [6] J. Theiler and D. Prichard, Physica D **110**, 221 (1996).
 [7] T. Schreiber, Phys. Rev. Lett. **80**, 2105 (1998).
 [8] T. Schreiber and A. Schmitz, Phys. Rev. Lett. **77**, 635 (1996).
 [9] T. Schreiber and A. Schmitz, Physica D **142**, 346 (2000).
 [10] C. Raeth and G. Morfill, J. Opt. Soc. Am. A **14**, 3208 (1997).
 [11] F. Jamitzky, R. Stark, W. Bunk, S. Thalhaammer, C. Raeth, T. Aschenbrenner, G. Morfill, and W. Heckl, Ultramicros. **86**, 241 (2000).
 [12] C. Raeth, W. Bunk, M. Huber, G. Morfill, J. Retzlaff, and P. Schuecker, MNRAS **337**, 413 (2002).
 [13] C. Raeth and P. Schuecker, MNRAS **344**, 115 (2003).
 [14] P. Grassberger, R. Badii, and A. Politi, J. Stat. Phys. **51**, 135 (1988).
 [15] T. Halsley, M. Jensen, L. Kadanoff, I. Procaccia, and B. Shraiman, Phys. Rev. A **33**, 1141 (1986).
 [16] H. Boehm, C. Raeth, R. Monetti, D. Mueller, D. Newitt, S. Majumdar, E. Rummeny, G. Morfill, and T. Link, Inv. Radiol. **38**, 269 (2003).
 [17] R. Monetti, H. Boehm, D. Mueller, D. Newitt, S. Majumdar, E. Rummeny, T. Link, and C. Raeth, Proc. SPIE: Med. Imag. **5032**, 1777 (2003).
 [18] C. Peng, S. Buldyrev, S. Havlin, M. Simons, H. Stanley, and A. Goldberger, Phys. Rev. E **49**, 1685 (1994).
 [19] C. Heneghan and G. McDarby, Phys. Rev. E **62**, 6103 (2000).
 [20] Proc. Int. Workshop on Econophysics & Stat. Finance, Physica A **269**, eds. R. Mantegna (Issue 1 1999).
 [21] D. Hsieh, J. Finance **46**, 1839 (1991).
 [22] T.-H. Lee, H. White, and C. Granger, J. Econometrics **56**, 269 (1993).
 [23] R. Mantegna and E. Stanley, Nature **376**, 46 (1995).
 [24] S. Ghashghaie, W. Breymann, J. Peinke, P. Talkner, and Y. Dodge, Nature **381**, 46 (1996).
 [25] R. Mantegna and E. Stanley, Nature **383**, 587 (1996).
 [26] This data set is freely available at <http://finance.yahoo.com/>.